

Characterization of the nanocryosurgical freezing process through modifying Mazur's model

Jing-Fu Yan¹ and Jing Liu^{1,2,a)}

¹*Technical Institute of Physics and Chemistry, Chinese Academy of Sciences, P.O. Box 2711, Beijing 100080, People's Republic of China*

²*Biomedical Engineering Department, School of Medicine, Tsinghua University, Beijing 100084, People's Republic of China*

(Received 7 October 2007; accepted 23 February 2008; published online 28 April 2008)

Nanoparticles enhanced freezing, termed as nanocryosurgery, is a newly emerging cryosurgical technique which has potential advantage in targeted tumor treatment. However, there are currently no models available to predict the effects of nanoparticles on cell-level biophysical events during cryosurgery. Here, we present a theoretical model through modifying Mazur's equation and ice nucleation theory to predict the kinetic course of the target cell such as water transport and ice nucleation during nanocryosurgical process. The transient temperature response of the target cell, which was a major influential variable of the model, was calculated by coupling the Pennes bioheat equation and the thermal conductivity model of nanoparticle-fluid mixture. With the model, the freezing effect of nanocryosurgical process on target cell at varying distances from cryoprobe can be comprehensively characterized from micro- to macroscale. Parametric studies revealed that the kinds of nanoparticles and their extracellular volume fraction are two important factors to affect cell-level freezing response compared with other factors such as the cell radius and intracellular volume fraction of nanoparticles. The corresponding sensitivity analysis of various parameters is also reported. This study would help to better understand the role of nanoparticles in the freezing process and benefit to optimize the protocol of tumor treatment when nanocryosurgery is administrated. © 2008 American Institute of Physics. [DOI: [10.1063/1.2910676](https://doi.org/10.1063/1.2910676)]

I. INTRODUCTION

Cryosurgery has become more and more popular owing to its specific advantages such as less invasive than conventional surgery; minimizing pain, bleeding, and other complications of surgery; and less expensive than other treatments and requiring a shorter recovery time and a shorter hospital stay.^{1,2} Although currently, it is still not a routine treatment protocol, it is rather rapidly developing as an alternative tumor therapy. A major concern involved in a cryosurgery is to maximize the efficiency of freezing to enhance cryodestruction to the targeted tissues. Along with the fast progress of nanotechnology in medical field, the nanoparticles involved cell freezing method was recently found highly useful in improving the freezing capability of a cryosurgery.

The earliest studies of using nanoparticles to enhance cryosurgery may be dated back to 2005.³⁻⁵ It was found that injecting certain high thermal conductivity nanoparticle solution into localized tissues could significantly improve the freezing rate, change the formation of iceball, and affect the growing direction of iceball there. In fact, noticing the particularity of nanoparticles, certain concerns are being focused on their unique applications in medicine. One of such endeavors is the nanohyperthermia which relies on using high temperature to destroy diseased tissues loaded with nanoparticles.⁶⁻⁸ As is gradually known, the nanoparticles induced hyperthermia has many additional advantages over

conventional heating protocol. It will not only evidently increase the curative effect of conformal treatment of tumors but also help deliver antineoplastic drug or angiogenesis to damage targeted tumors combined with surgery.^{9,10} Obviously, such benefits can also be anticipated when introducing nanoparticles to cryosurgery.

In order to better understand the thermal and kinetic behaviors in both tissue and cellular level during a nanocryosurgical treatment, it is imperative to establish a theoretical model for characterizing such freezing process. At present, the most commonly used model predicting the cell volumetric change is developed by Mazur. Based on this classical model, the well known two factor hypotheses¹¹ were proposed to describe the biophysical responses coupled to tissue injury during freezing process. Cell dehydration and intracellular ice formation (IIF) are two major factors which have been proven and recognized as an important mechanism to explain cell injury as a result of the freezing process.¹²⁻¹⁷ However, until now, no existing model can be directly adopted to predict the dynamics of both the thermal conditions inside frozen tissue and cellular-level biophysical events when nanoparticles are loaded into tissues and cells. For such reason, a modified Mazur's model is developed in this paper to probe into the biophysical events such as water transport (or cell volumetric change) and IIF, experienced by cells with nanoparticles during freezing. The Pennes bioheat equation using effective heat capacity¹⁸ as a governing equation is applied to describe the phase change process of tissues during cryosurgery. For unfrozen particle embedded tissues, a model of the effective thermal conductivity of

^{a)}Author to whom correspondence should be addressed. Electronic mail: jliu@cl.cryo.ac.cn. Tel.: +86-10-82543765. FAX: +86-10-82543767.

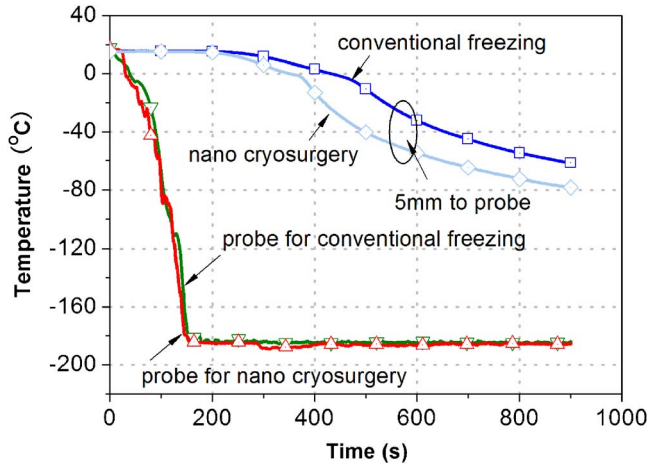


FIG. 1. (Color online) Transient temperature response at measurement positions with or without nano-Ag on pork tissues.

nanoparticle-fluid mixture which considers the effects of nanolayer thickness, nanoparticle size, and volume fraction is adopted.¹⁹ On the other hand, the Hamilton–Crosser model²⁰ is applied to calculate the effective thermal conductivity of frozen particle embedded tissues. The modified model and numerical results are expected to provide valuable information to optimize the protocol of nanocryosurgery.

II. TYPICAL EXPERIMENTS ABOUT NANOCRYOSURGERY

To assess the influence of nanoparticles upon freezing effects, two *in vitro* experimental results were presented in this paper. What were depicted in Fig. 1 were typical temperature response curves of pork tissues when subjected to freezing by one cryoprobe, either loading with or without nano-Ag, respectively. The measurement point is at one place away from the probe tip by 5 mm. Moreover, 20 ml particulate suspension (5 mg/ml) is directly injected by syringe into the sample surrounding the probe. It can be found that the lowest temperature at the selected position for the case of injecting nano-Ag can reach -80°C , which is much lower than its counterpart case without injection. Meanwhile, the freezing rate was also comparatively increased at the measurement position where nano-Ag was locally injected. This was owed to the enhanced heat conduction due to addition of metal nanoparticles into tissues. Figure 2 shows the thermal image for temperature distribution on pork tissues injected with different volumes of particulate solution.³ We injected aqueous suspension of nanoaluminum in water clockwise from sign 1 to sign 4 at the same distance from the cryoprobe. The volumes for the injection are 1, 2, 3, and 4 ml. Clearly, as revealed by the thermal images, different doses of injecting solution have resulted in various magnitudes on iceball formation. The more volume for the solution to be injected, the more possible the iceball will grow fast toward that direction. Additional experimental measurements on using nano particle to enhance tissue freezing can also be found from our previous work.⁴ Readers are referred there for further information. For brevity, they will not be provided here.

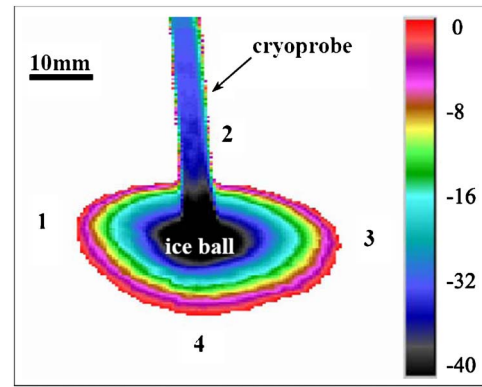


FIG. 2. (Color online) Thermal image for temperature distribution on pork tissues injected with 1, 2, 3 and 4 ml (from signs 1 to 4) aqueous suspension of nanoaluminum, respectively.

III. THEORETICAL MODEL

A. Bioheat transfer model in tissue level

Nanoparticle enhanced cryosurgery can produce a predictable improvement of temperature response on the target cell or tissue. In the theoretical model, as established below, a 5 mm probe was considered and perpendicularly inserted into the tissues. The computational domain is schematically shown in Fig. 3. Due to the symmetric feature of the space, the three-dimensional geometry can be reduced to a two-dimensional domain in a cylindrical coordinate system. In addition, considering the extremely small volume of a single cell compared to that of the whole tissue, each point of the computational domain is assumed to be a target cell whose volume can be ignored while the temperature can be regarded as the lumped one in the heat transfer model. The uniform governing equation during cryosurgery can be written as¹⁸

$$\tilde{C} \frac{\partial T}{\partial t} = \tilde{K} \left(\frac{\partial^2 T}{\partial r^2} + \frac{1}{r} \frac{\partial T}{\partial r} + \frac{\partial^2 T}{\partial z^2} \right) + \tilde{\omega}_b C_b (T_a - T) + \tilde{Q}_m, \quad (1)$$

where $T(r)$ is the lumped cell temperature at the position r ; C_b , $\tilde{\omega}_b$ are the heat capacity and the blood perfusion of biological tissues, respectively; \tilde{K} , \tilde{C} are the equivalent thermal conductivity and heat capacity of biomaterial which has included contribution of the loaded nanoparticles; respectively, \tilde{Q}_m is the equivalent metabolic heat generation; and T_a is the arterial temperature. Since the phase change of real biological tissue does not take place at a fixed temperature but within a temperature range, it is reasonable to substitute a large effective heat capacity over a temperature range (T_{ml}, T_{mu}) for the latent heat, where T_{ml} and T_{mu} are the lower and upper phase transition temperatures of the tissue, respectively. The specific definitions of those equivalent parameters are given as follows:

$$\tilde{C}(T) = \begin{cases} C_f, & T < T_{ml} \\ \frac{Q_l}{T_{mu} - T_{ml}} + \frac{C_f + C_u}{2}, & T_{ml} \leq T \leq T_{mu} \\ C_u, & T > T_{mu} \end{cases}, \quad (2)$$

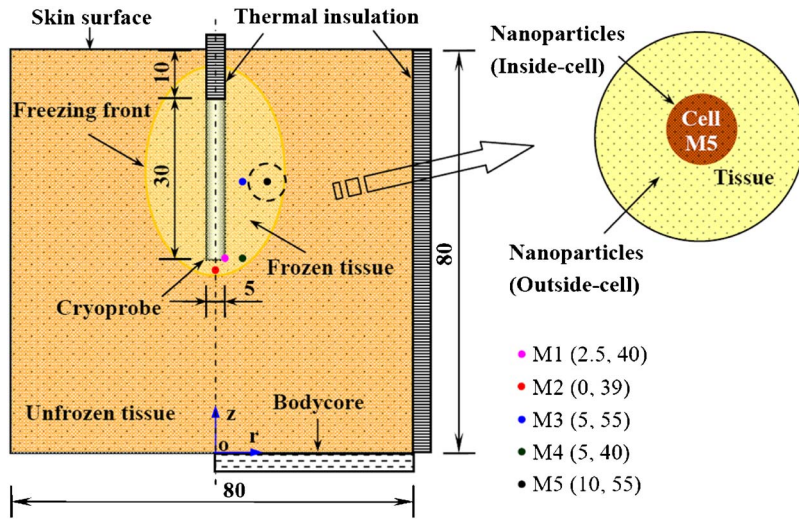


FIG. 3. (Color online) Schematic for computational domain when nanoparticles are embedded into tissues during freezing procedure (not to scale).

$$\tilde{K}(T) = \begin{cases} K_f, & T < T_{ml} \\ \frac{K_f + K_u}{2}, & T_{ml} \leq T \leq T_{mu} \\ K_u, & T > T_{mu} \end{cases}, \quad (3)$$

$$\tilde{Q}_m(T) = \begin{cases} 0, & T \leq T_{mu} \\ Q_m, & T > T_{mu} \end{cases}, \quad (4)$$

$$\tilde{\omega}_b(T) = \begin{cases} 0, & T \leq T_{mu} \\ \omega_b, & T > T_{mu} \end{cases}, \quad (5)$$

where subscripts f and u represent frozen and unfrozen mixture, respectively; C_f , C_u are the effective thermal capacity; K_f , K_u are the effective thermal conductivity; and Q_m is the metabolic heat generation.

The heat transfer model employed here is based on three principal assumptions: (1) the spatial temperature variation within the cell is omitted for simplicity; (2) cell is regarded as ideal sphere and the mediums embedded with nanoparticles are homogeneous; and (3) the thermal properties of nanoparticles are treated as temperature independent.

The condition at the boundary of cylindrical calculation domain is prescribed as follows:

$$\frac{\partial T}{\partial r} = 0 \quad (\text{symmetric axis in tissue}), \quad (6)$$

$$\frac{\partial T}{\partial r} = 0 \quad (\text{insulation wall of probe and both sides of tissue}), \quad (7)$$

$$T = 310 \text{ K} \quad (\text{body core}), \quad (8)$$

$$T = \begin{cases} -(310 - 77)/180 \times t + 310, & t < 180 \text{ s} \\ 77, & 180 \text{ s} \leq t \leq 1200 \text{ s} \end{cases} \quad (\text{working part of probe}), \quad (9)$$

$$-k \frac{\partial T}{\partial z} = h_f(T_f - T) \quad (\text{skin surface}), \quad (10)$$

where h_f is the convective heat transfer coefficient between the environment and the surface and T_f is temperature of the surrounding air. The initial temperature field in tissue is $T = 310 \text{ K}$.

Considering the energy equation for a binary system (biology part and nanoparticle part), the effective thermal capacity is determined by the volume fraction of particle α_0 outside the cell and reads in the following forms:

$$C_f = C_{ft}(1 - \alpha_0) + C_p \alpha_0, \quad (11)$$

$$C_u = C_{ut}(1 - \alpha_0) + C_p \alpha_0, \quad (12)$$

where the subscripts ft and ut mean frozen and unfrozen pure tissues, respectively. Subscript p stands for the loaded nanoparticles.

As for the effective thermal conductivity of unfrozen particle embedded tissue, a model¹⁹ which had included the

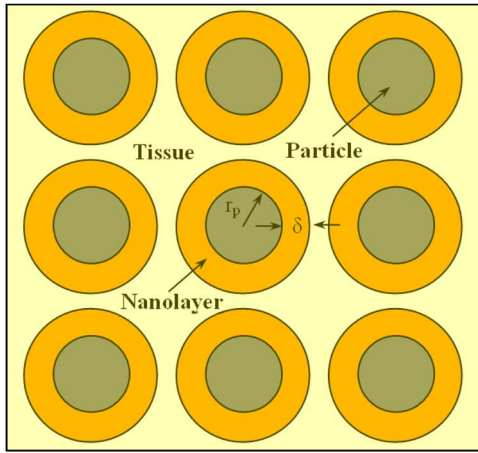


FIG. 4. (Color online) Schematic structures for nanoparticle and its interfacial nanolayer in a homogeneous nanofluid.

effects of nanolayer thickness, nanoparticle size, volume fraction, and different kinds of nanoparticles is adopted in this study. Figure 4 denotes the schematic structures of the model. The final expression of effective thermal conductivity in unfrozen area is set as

$$K_u = \left(3\Theta\alpha_T + \frac{3\Theta^2\alpha_T^2}{1-\Theta\alpha_T} + 1 \right) k_{ut}, \quad (13a)$$

with

$$\Theta = \frac{\beta_{fl}[(1+\gamma)^3 - \beta_{pl}/\beta_{fl}]}{(1+\gamma)^3 + 2\beta_{fl}\beta_{pl}}, \quad (13b)$$

where α_T is the total volume fraction of the original nanoparticle and nanolayer; γ is the ratio of the nanolayer thickness to the original particle radius; β_{fl} , β_{pl} , β_{pl} are the ratio coefficient of thermal conductivities of the nanofluid, nanolayer, and nanoparticles, respectively. For brevity, we will not discuss this model here. Readers are referred to Ref. 19 for more details.

As for the effective thermal conductivity of frozen particle embedded tissue, Hamilton–Crosser (HC) model in which nanoparticles are all treated as ideal spheres is used and depicted as²⁰

$$K_f = k_{ft} \frac{k_p + 2k_{ft} - 2\alpha_0(k_{ft} - k_p)}{k_p + 2k_{ft} + \alpha_0(k_{ft} - k_p)}, \quad (14)$$

where k_p and k_{ft} are thermal conductivities of nanoparticles and frozen pure tissues, respectively.

B. Mathematical model of water transport in cellular level

In 1963, Mazur proposed a two-compartmental, lumped parameter model to quantitatively describe the dehydration course of cells during freezing process.¹¹ The intra- and extracellular compartments were assumed to be well mixed and separated by a semipermeable membrane which only admitted transport of water. However, due to the introduction of nanoparticles, Mazur's model may not accurately predict the water transport across the cell membrane during freezing

process. For this reason, a modified Mazur's model is proposed in a system comprising a biological cell with implanted nanoparticles and extracellular ice.

In Mazur's membrane-limited transport model, the molar flux of water from the intracellular to the extracellular compartment was given by¹¹

$$J_w = \frac{L_0\Delta\mu}{\nu_w^2} \exp\left[-\frac{E_0}{R_g}\left(\frac{1}{T} - \frac{1}{T_0}\right)\right], \quad (15)$$

where L_0 is the reference membrane water permeability; E_0 is the activation energy; R_g is universal gas constant; T_0 is the equilibrium freezing temperature of water; ν_w is the molar specific volume of water; and $\Delta\mu = \mu_{ice} - \mu_w$, which is the chemical potential difference across the membrane. μ_{ice} is the chemical potential of extracellular ice and μ_w is the chemical potential of water at the intracellular surface of the cell membrane. The water chemical potential difference is a result of depletion of extracellular water by ice formation.

As water leaves the cell, the cell will shrink. The rate of change of the cell volume can be expressed as

$$\frac{dV}{dt} = 4\pi R^2 \frac{dR}{dt}, \quad (16)$$

where t is time and R is the cell radius. Because the intracellular fluid is incompressible, volume changes are caused only by the transmembrane water flux. Thus, continuity requires that

$$\frac{dR}{dt} = -J_w \nu_w. \quad (17)$$

With the assumption that the extracellular environment consists of ice and unfrozen aqueous solution in mutual equilibrium, the chemical potential of the extracellular water can be determined from the Clausius–Clapeyron relationship, yielding¹¹

$$\mu_{ice} = \mu_0 + \Delta H_f \left(\frac{T}{T_0} - 1 \right), \quad (18)$$

where μ_0 is the chemical potential of water at T_0 and ΔH_f is the molar specific heat of fusion of water.

If one approximates the cytosol-nanoparticle mixture as an ideal solution, Raoult's law can be used to approximate the chemical potential of the intracellular water,

$$\mu_w = \mu_0 + R_g T \ln(\chi_w), \quad (19)$$

with

$$\chi_w = \frac{C_w}{C_w + \sigma_s C_s}, \quad (20)$$

where $\sigma_s=2$ represents the salt dissociation constant and χ_w is the mole fraction of intracellular water. Considering the hypothesis that C_w is uniform and water is the only species that can be transferred across the cell membrane, there is a one-to-one correspondence between the intracellular water concentration and the cell volume V_c

$$C_w = \frac{(V_0 - V_b - V_p)C_{w0}\nu_w - (V_0 - V_c)}{(V_c - V_b - V_p)\nu_w}, \quad (21)$$

where V_0 and C_{w0} are the initial values of V_c and C_w , respectively; V_b is the osmotically inactive volume; and V_p is the total volume of nanoparticles loaded in cell.

According to the equations as mentioned above, the modified Mazur's equation can be given as follows:

$$\frac{dV_c}{dt} = -\frac{L_p(36\pi V_c^2)^{1/3}R_gT}{\nu_w} \left[\frac{\Delta H_f}{R_g} \left(\frac{1}{T_0} - \frac{1}{T} \right) - \ln \left(\frac{V_c - V_b - V_p - C_{s0}\nu_s(V_0 - V_b - V_p)}{V_c - V_b - V_p - C_{s0}(\nu_s - \sigma_s\nu_w)(V_0 - V_b - V_p)} \right) \right] \quad (22)$$

C. Ice nucleation model

The number of intracellular ice nuclei as a function of time follows a stochastic process as expressed by

$$\bar{N}(t) = \int_0^t n(t)dt, \quad (23)$$

where n is the average nucleation rate of a cell. A detailed treatment of the stochastic behavior of the intracellular crystal growth is beyond the scope of this study. More explanations on $\bar{N}(t)$ can be found elsewhere.²¹

The average nucleation rate n is a function of temperature and cytoplasm composition. By applying the Eyring reaction rate theory, n can be described as

$$n(c, T) = \Omega(c, T) \exp[-\kappa'(c, T)\tau(c, T)], \quad (24)$$

where, Ω and κ' are the kinetic and thermodynamic coefficients, respectively. The value of κ' is cell type-dependent constant. Due to limitation of data source, it was set to 1.5 (1–2) in this study. Further, one has $\tau(c, T) = T_m^5(T_m - T)^{-2}T^{-3}$ in which the equilibrium melting point T_m reads as follows:

$$T_m = \left(\frac{1}{T_0} - \frac{R_g}{\Delta H_f} \ln \chi_w \right)^{-1}. \quad (25)$$

The nucleation coefficient Ω , which depends on concentration and temperature, can be estimated by scaling²¹

$$\Omega(c, T) = \Omega_0 \left[\frac{\eta_0}{\eta(c, T)} \right] \left(\frac{T}{T_{h0}} \right)^{1/2} \left(\frac{c_w}{c_{w0}} \right), \quad (26)$$

where T_{h0} is the homogeneous nucleation temperature for pure water.

In addition, the hard-sphere model^{22,23} can be used to calculate the volume fraction of the rigid spheres ϕ_s , which is used to estimate the viscosity η of the intracellular solution in this study. That is,

$$\eta(c, T) = 0.139(10^{-3}) \left[\frac{T}{225} - 1 \right]^{-1.64} \exp \left[\frac{2.5\phi_s}{1 - Q\phi_s} \right], \quad (27)$$

where $Q=0.609375$ represents the hydrodynamic interaction constant. Considering the hard spheres will comprise hy-

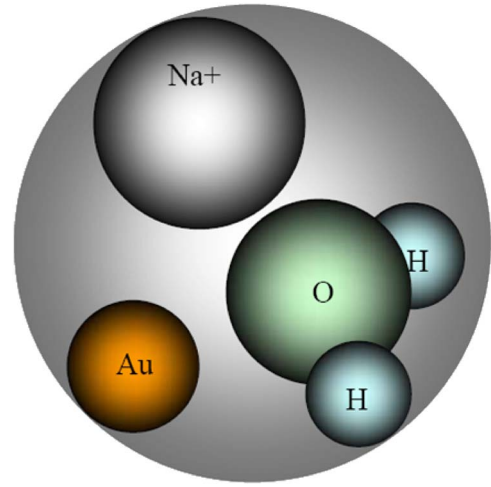


FIG. 5. (Color online) Illustration of ϕ_s containing NaCl, one water molecule and one nano-Au.

drated ions and nanoparticles, as shown in Fig. 5, ϕ_s can be given as

$$\phi_s = C_s[\nu_s + h\nu_w + h'\nu_p], \quad (28)$$

where C_s is the salt concentration; ν_s , ν_p are the molar specific volume of salt and nanoparticles, respectively; h is the effective number of water molecules in the hydration shell and was set to typical value 1; h' is the coefficient of nanoparticles in the hydration shell and was set to 0.5 when using nano-Fe₃O₄ particle, or 1 when using nano-Ag or nano-Au particle.

All of the necessary thermophysical, biophysical, and geometric constants and parameters are summarized in Tables I and II. The structural and biophysical characteristics of rat embryos were used for the tissue medium and the corresponding parameters can be found in Refs. 21, 23, and 24

TABLE I. Thermophysical properties of biological tissues and nanoparticles.

Properties	Units	Values
Thermal conductivity of frozen tissue, k_{ft}	W/m °C	2.0
Thermal conductivity of unfrozen tissue, k_{ut}	W/m °C	0.5
Thermal conductivity of Fe ₃ O ₄ , k_p	W/m °C	7.1
Heat capacity of Fe ₃ O ₄ , C_p	J/m ³ °C	3.2×10^6
Thermal conductivity of Au, k_p	W/m °C	297.7
Heat capacity of Au, C_p	J/m ³ °C	2.2×10^6
Thermal conductivity of Ag, k_p	W/m °C	417.5
Heat capacity of Ag, C_p	J/m ³ °C	2.5×10^6
Heat capacity of frozen tissue, C_{ft}	J/m ³ °C	2.0×10^6
Heat capacity of blood, C_b	J/m ³ °C	3.6×10^6
Heat capacity of unfrozen tissue, C_{ut}	J/m ³ °C	3.6×10^6
Lower phase transition temperature of tissue, T_{ml}	K	265
Higher phase transition temperature of tissue, T_{mu}	K	272
Metabolic rate of unfrozen tissue, Q_m	W/m ³	4200
Arterial temperature, T_a	K	310
The molar specific heat of fusion of water, ΔH_f	J/mol	6017

TABLE II. Parameter values used in the model.

Items	Units	Values
Initial cell volume, V_0	m^3	2.62×10^{-13}
Osmotically inactive volume, V_b	m^3	5.58×10^{-14}
Intracellular volume fraction, α_i	\dots	0.02
Extracellular volume fraction, α_0	\dots	0.01–0.2
Occupied volume by nanoparticle, V_p	m^3	$V_0 \cdot \alpha_i$
Nanolayer of thickness, δ	m	2.0×10^{-9}
Radius of nanoparticle, r_p	m	$0.6 \times 10^{-8} - 1.0 \times 10^{-8}$
The molar specific volume of salt, ν_s	m^3/mol	2.7×10^{-5}
The molar specific volume of water, ν_w	m^3/mol	1.8×10^{-5}
The molar specific volume of nanoparticle, ν_p	m^3/mol	4.55×10^{-5} (Fe_3O_4) 1.03×10^{-5} (Ag) 1.02×10^{-5} (Au)
Initial salt concentration, C_{s0}	mol/m^3	142
Initial water concentration, C_{w0}	mol/m^3	55343
Membrane permeability reference value, L_0	$\text{m}^2 \text{ s}/\text{kg}$	4.77×10^{-13}
Membrane permeability activation energy, E_0	J/mol	5.3×10^4
Reference temperature, T_0	K	273
Homogeneous nucleation temperature for pure water, T_{h0}	K	235
Nucleation rate kinetics coefficient, Ω_0	$\text{s}^{-1}\text{m}^{-3}$	2×10^{50}

IV. RESULTS AND DISCUSSION

Figure 6 shows the influence of various volume fraction of nano-Ag on the temperature profile of tissue and the formation of iceball at $t=1200$ s. The temperature contour lines for $T=233$ K, $T=T_{ml}$ (265 K), and $T=T_{mu}$ (272 K) differentiate between the effective killing zone, mushy zone and unfrozen zone, respectively. It can be seen that once nano-Ag is loaded, the size of iceball becomes enlarged than that of no particle case. The higher volume fraction of nano-Ag is, the larger volume of iceball can be formed. If contour line of T_{mu} is regarded as the edge of iceball in Fig. 6(c), the length of maximum semiaxis of iceball along r and z directions can, respectively, reach 0.033 and 0.06 m, which are about 27% and 7% increases compared to Fig. 6(a). The corresponding effective killing area and mushy zone are also enlarged with the increase of volume fraction of nano-Ag. Therefore, it can be found that nanoparticles are beneficial to increase the volume of iceball as well as extend the frozen injury zone.

Figures 7(a)–7(f) give the transient temperature re-

sponses of cell at measurement points during freezing process and their corresponding transient cell volume responses, which reflect the influence of volume fraction of nano-Ag on the biophysical events at different target cell during freezing process. It can be seen that, for M5, the predicted results show good accordance with the currently available experimental data, as shown in Fig. 1. Moreover, for each measurement point (M2–M5) in Figs. 7(c) and 7(e), the freezing rate becomes higher and the end temperature is lower than that of no particle case, as shown in Fig. 7(a). Such thermal dynamic change has a strong effect on the water transport process of the target cell. With the increase in freezing rate at the target cell, the time for water transport process to reach the new equilibrium state is greatly shortened, and thus, the final cell volume [shown in Figs. 7(d) and 7(f)] is larger than that of no particle case [shown in Fig. 7(b)]. At the position of M5, for no particle case, the time of water transport process is 700 s and the final cell volume is $2.24 \times 10^{-13} \text{ m}^3$. However, when the extracellular volume fraction of nano-Ag

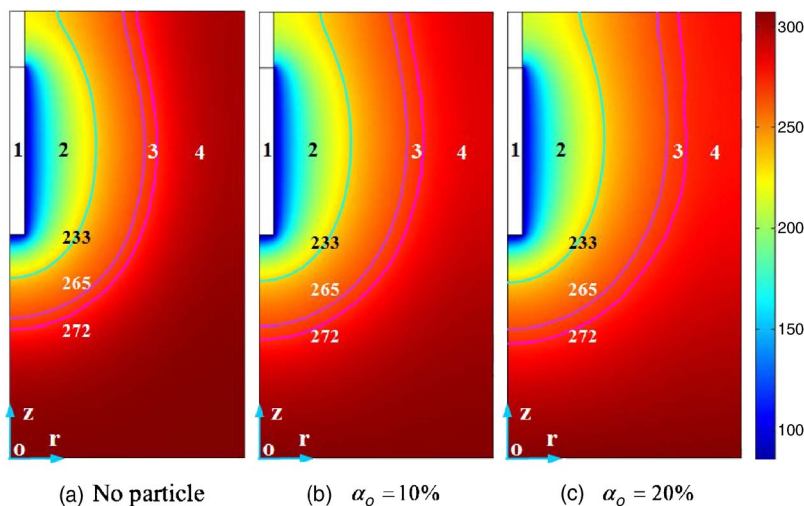


FIG. 6. (Color online) Effects of various volume fractions of nano-Ag on the temperature profile of tissue and the formation of iceball at $t=1200$ s. (1) Cryo-probe; (2) effective killing zone; (3) mushy zone; and (4) unfrozen zone.

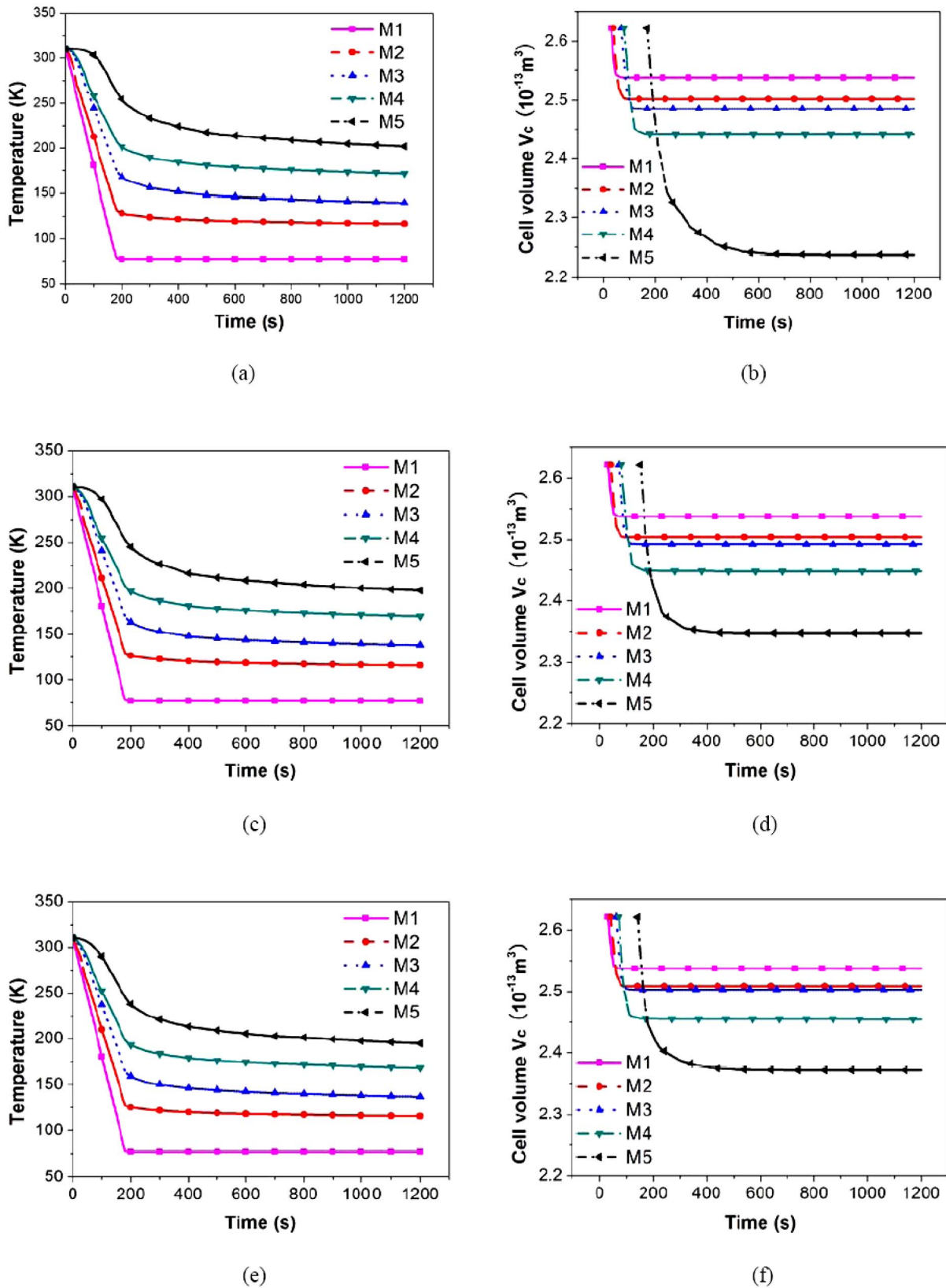


FIG. 7. (Color online) The transient temperature responses of cell at measurement points during freezing procedure and their corresponding transient cell volume response during freezing procedure [(a) and (b)] without nano-Ag; [(c) and (d)] nano-Ag, $\alpha_i=2\%$, $\alpha_0=10\%$, $r_p=1 \times 10^{-8}$ m; and [(e) and (f)] nano-Ag, $\alpha_i=2\%$, $\alpha_0=20\%$, $r_p=1 \times 10^{-8}$ m.

reaches 20% ($\alpha_0=20\%$), as shown in Fig. 7(f), the time for water transport process to reach equilibrium can be reduced to 500 s and the final cell volume is found to be kept at

$2.37 \times 10^{-13} \text{ m}^3$. Therefore, it can be indicated that for the same distance from the probe, the freezing effect of nanoparticles case on target cell is much stronger than that of no

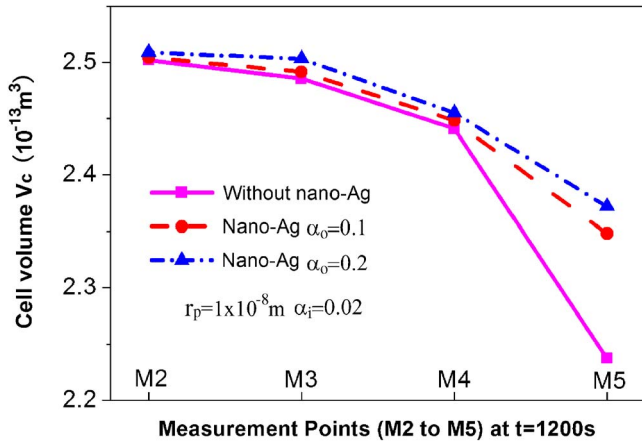


FIG. 8. (Color online) The final cell volume at each measurement points (M2–M5) with different volume fractions α_0 of nano-Ag at $t=1200$ s ($r_p = 1 \times 10^{-8}$ m, $\alpha_i = 2\%$).

particle case. That is to say, it is feasible to enhance freezing effects of conventional cryosurgery by using nanoparticles. In addition, Fig. 8 shows the final cell volume of each measurement points (M2–M5) with different volume fractions of nano-Ag at $t=1200$ s. It is clearly seen that once the volume fraction of nano-Ag increased, its influence on the target cell far from the probe could be stronger than the one near the probe and this could be useful to improve killing effects of the cells far away from the probe.

Figure 9 reflects the influence of various kinds of nanoparticles on the thermal history of the cell (M5) and its corresponding volume response during freezing process. It can be easily seen that various kinds of nanoparticles result in different transient temperature profiles which leads to different water transport processes. The reason lying in those various kinds of nanoparticles leads to different thermal conductivities of particle-tissue mixtures which create different thermal dynamics. Consequently, the whole water transport process which has a close relationship with the characteristic temperature T would be different. The higher value of thermal conductivity of nanoparticles is the higher value of final cell volume will be. From Fig. 9(b), it can be concluded that the nano-Ag which has the highest thermal conductivity

value produces much more influence on freezing process as well as water transport process of target cell than that by nano-Au or nano-Fe₃O₄.

Figure 10 shows the influence of different radius of the same nanoparticles on thermal history of the cell (M5) and its corresponding volume response during freezing process. Figure 10(b) illustrates that the final cell volume will increase with the increasing radius of nano-Au. However, such effect is not very much strong compared to the volume fraction of nano-Au. The relative change (increase) in the final cell volume is only about 0.4% when the radius increases from 6×10^{-9} to 1×10^{-8} m.

Figure 11 shows the effect of various kinds of nanoparticles on cell (M5) nucleation rate during freezing process. The case of nano-Ag has the shortest time (650 s) to reach maximum nucleation rate ($5.82 \times 10^{-31} \text{ m}^{-3} \text{ s}^{-1}$) while the case of no particles has the longest one (1150 s). Therefore, it can be seen that, at the same position, intracellular ice formation happens earlier in the cell with nanoparticles than the one without nanoparticles. In addition, various kinds of nanoparticles have different influences on the IIF of the target cell. From Fig. 11, it can be observed that IIF is mainly dependent on the thermal history of the cell. The cell with nano-Ag which results in the fastest freezing process leads to the earliest IIF. However, a faster freezing process does not necessarily leads to an earlier IIF. When comparing nano-Fe₃O₄ case with nano-Au case, the cell with nano-Fe₃O₄ results in an earlier IIF than the one with nano-Au, although the freezing rate of the latter case is higher than the former one. The reason lies in that nano-Fe₃O₄ has a high ν_p which has more influence on the nucleation rate than the characteristic temperature T . Therefore, it can be said that some characteristic features of nanoparticles can also play important role along with characteristic temperature T to influence the IIF which is commonly believed as the major factor leading to irreversible damage to the cell. If proper characteristic features of nanoparticles are taken in cryosurgery, it is possible to realize the maximum killing effect.

From the above simulation, it can be readily concluded that nanocryosurgery has stronger freezing effects than that of conventional one. By taking full use of this advantage, some insufficient freezing area usually occurred when treating

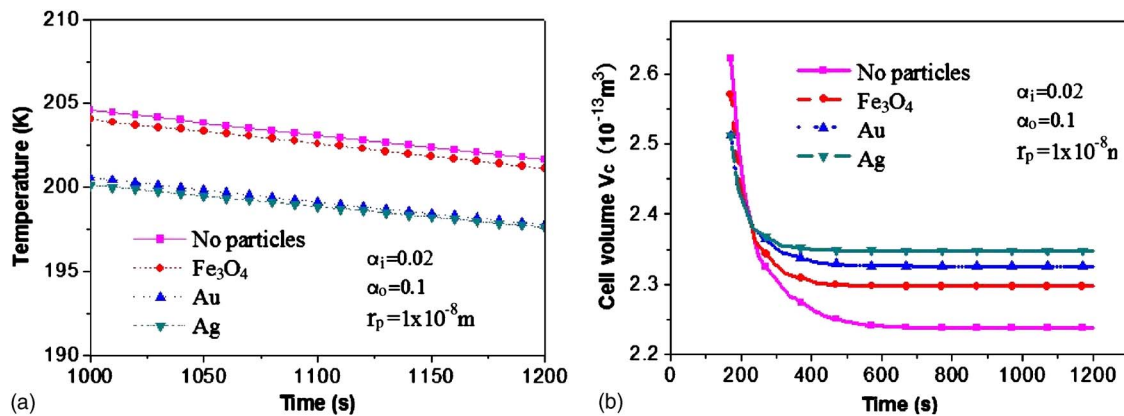


FIG. 9. (Color online) (a) The transient temperatures and (b) volume responses of cell (M5) during freezing procedure for different kinds of nanoparticles with same radius $r_p = 1 \times 10^{-8}$ m when the intracellular volume friction of particles is $\alpha_i = 2\%$ and outside-cell one is $\alpha_0 = 10\%$, respectively.

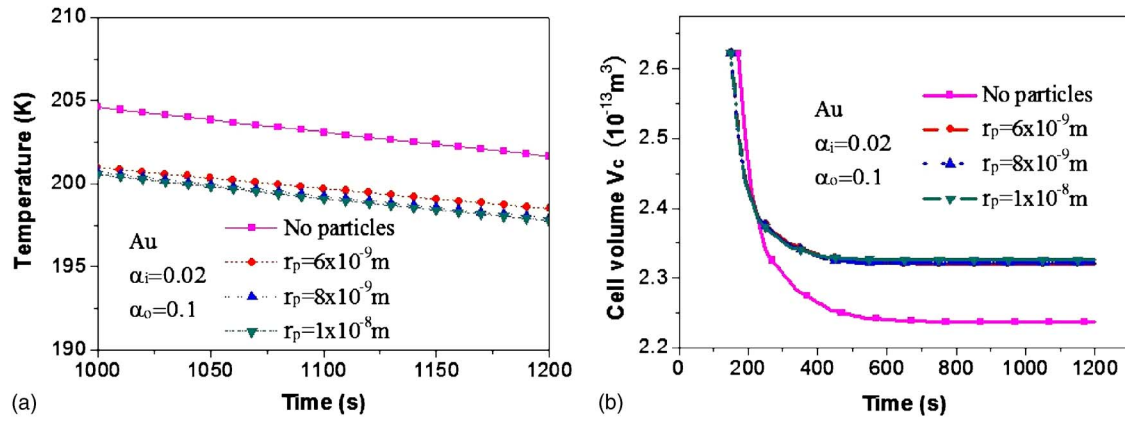


FIG. 10. (Color online) (a) The transient temperature and (b) volume responses of cell (M5) during freezing procedure when the intracellular volume fraction of nano-Au is $\alpha_i=2\%$ and outside-cell one is $\alpha_o=10\%$, respectively.

large tumors in a conventional cryosurgery could be prevented. In addition, it can be found that when nanoparticles are introduced into tumor cells, they would result in an earlier IIF which could accelerate the death of the target cells. On the other hand, using nanoparticles as seeds, heterogeneous nucleation rate could be significantly improved. This will help to dramatically increase the possibility of nucleation in cells, which in turn results in a higher probability of IIF leading to a lethal killing of tumor cells. Thus, it may be concluded that the use of nanoparticles in cryosurgery is feasible and could serve as an effective supplement to the conventional cryosurgery.

V. SENSITIVITY ANALYSIS OF MODEL PARAMETERS

Efforts made in this paper provide the first theoretical interpretation on the detailed events occurred in a nanocryosurgical process. However, it should be pointed out that the predicted results are sensitive to the values of some important model parameters of nanoparticles such as α_o , α_i , r_p , h' , etc. Besides, the nanoparticles that could be loaded inside the target cells may depend on the particle type and cellular environment. To address such issue, a sensitivity analysis is also performed in this study to identify and rank the most influential variables in the model. It is a routine procedure in estimating the change in the output with respect to changes in only one input parameter.²⁵ With all other parameters held constant, this one-dimensional analysis assumes that the input parameters are independent of each other. This is usually not the case when considering the complex relationships in the thermal-kinetic coupled system. However, this method allows the identification of those parameters which have a crucial impact on the model predictions. The sensitivity measure is based on the deterministic sensitivity concept formulated by McCuen,²⁵ which is defined by the following expression:

$$S = \frac{O_2 - O_1}{O_{12}} \bigg/ \frac{I_2 - I_1}{I_{12}}, \quad (29)$$

where S is dimensionless sensitivity measure; I_1 and I_2 are the least and greatest input values, respectively; O_1 and O_2 are the corresponding outputs of argument I_1 and I_2 , respectively; I_{12} is the average of I_1 and I_2 ; and O_{12} is the average

of O_1 and O_2 . As it is the primary purpose of using the effective thermal conductivity model and HC model to illustrate the influence of nanoparticles on the thermal conductivity of binary system, the thermal conductivity of particle-tissue mixture (including unfrozen part and frozen part) was chosen as the output parameter from which the sensitivity measure was calculated. Table III lists the sensitivity analysis of the main input parameters. The compilation shows that most of those parameters of nanoparticles influence the thermal conductivity. Extracellular volume fraction α_o , as one of the input parameters, has the highest impact on the model predictions. Another important output parameter which reflects the influence of nanoparticles on freezing dynamics is the nucleation rate. Considering the high complexity and apparent nonlinear behavior of the nucleation rate as output parameter, only some typical input parameters were considered to calculate the sensitivity measure for the characteristic interval but not the entire input-output range. Since the input parameters are highly dependent of each other, for simplicity, we define the range of temperature T and cell volume V_c according to the freezing process of cell (M5) with nano-Ag. The specific main input parameters with sensitivity S are listed in Table IV. It can be seen that T has the highest

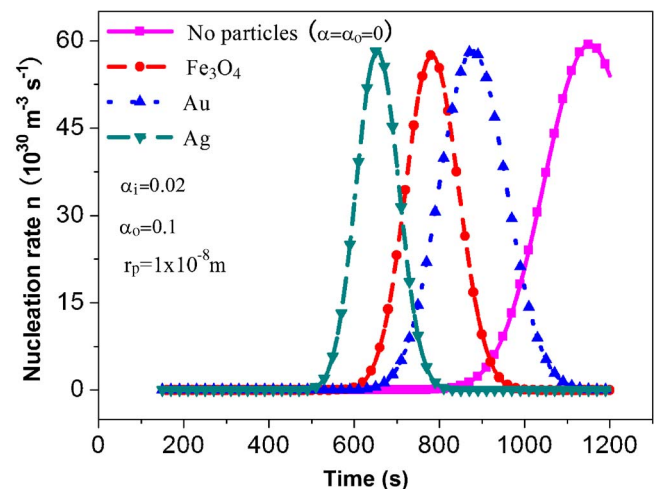


FIG. 11. (Color online) Effect of various kinds of nanoparticles on cell (M5) nucleation rate during freezing procedure.

TABLE III. Sensitivity analysis of the thermal conductivity of particle-tissue mixture.

Parameter	Unit	Range	S1 (unfrozen part)	S2 (frozen part)
Extracellular volume fraction, α_0	...	0.0–0.2	0.49	0.27
Radius of nanoparticle, r_p	m	6.0×10^{-9} – 10.0×10^{-9}	–0.09	0
Thermal conductivity of particles, k_p	W/m $^\circ$ C	5.0–2000	0.08	0.08

sensitivity value, the next is α_i , h' , V_c , and κ' are the input parameters to which the ice nucleation rate is less sensitive. According to the calculation, the parameters of nanoparticles which are related to thermodynamics are more influential to the model than other parameters of nanoparticles. However, it should be noted that since the sensitivity analysis method as adopted in this study is highly sensitive to the input range, the sensitivity values of some input parameters could be various with different input conditions. Clearly, further cellular level experimental justifications of the temperature and concentration dependence of these parameters are crucial to improve model accuracy. This needs further work in the near future.

VI. CONCLUSION

In this study, through incorporating the nanoparticle terms into Mazur's equation and combining with the Pennes bioheat model, the classical equations are modified to be capable of predicting the thermal dynamics of the cell and the cell-level biophysical events such as IIF when nanoparticles are involved during cryosurgery. Some conclusions from the present parametric analysis can be drawn as follows. First, nanoparticles involved cryosurgery could enhance the freezing effect and speed up the water transport process which results in an earlier intracellular ice nucleation on the target cell compared with conventional cryosurgery. Second, different kinds, radius, and volume fraction of nanoparticles have different influences on the cell freezing process. The larger thermal conductivity of nanoparticle, the more extent of enhancement of the cell freezing will be. In this way, although only three well biocompatible particles are proposed in calculation, some other nanomaterials with a higher thermal conductivity such as carbon nanotubes are expected to produce stronger effects on cell freezing response and damage to the target cells. Lastly, compared to

intracellular volume fraction and radius of nanoparticles, the extracellular volume fraction and kinds of nanoparticles play more important roles in the freezing process and ice nucleation process. The reason for the capability of accommodating nanoparticles by cell is limited which results in a low intracellular volume fraction. And thus, it produces a little effect on the viscosity η and water concentration C_w which have close relationship with the IIF. In the present study, the thermal dynamics of the cell during the freezing process is mainly determined by the high effective thermal conductivity of the outside cell environment due to high value of extracellular volume fraction of nanoparticles and their high thermal conductivity. Therefore, they have more effect on the biophysical events induced by the thermal history. In general, the present model could provide important information for the nanoparticles involved freezing process and serve as guidance for future nanocryosurgery.

ACKNOWLEDGMENTS

This work was partially supported by a NSFC Grant No. 50575219 and Dr. Shun-De Wu's Foundation of Tsinghua University.

TABLE IV. Sensitivity analysis of the ice nucleation rate.

Parameter	Unit	Range	S
Intracellular volume fraction, α_i	...	0.0–0.02	0.04
The coefficient of nanoparticles in the hydration shell, h'	...	0.0–3.0	0.008
Thermodynamic coefficient, κ'	...	1.0–2.0	0
Temperature, T	K	273–195	–0.72
Cell volume, V_c	m 3	2.62×10^{-13} – 2.37×10^{-13}	–0.002

- ¹A. A. Gage, *Surg. Gynecol. Obstet.* **174**, 73 (1992).
- ²B. Rubinsky, *Annu. Rev. Biomed. Eng.* **2**, 157 (2000).
- ³J. F. Yan, J. Liu, and Y. X. Zhou, 27th Annual International Conference of the IEEE Engineering in Medicine and Biology Society (EMBS), 2005 (unpublished), Vol. 4, p. 3559.
- ⁴T. H. Yu, J. Liu, and Y. X. Zhou, *Cryobiology* **50**, 174 (2005).
- ⁵Z. S. Deng and J. Liu, *Cryobiology* **50**, 183 (2005).
- ⁶S. A. Wickline and G. M. Lanza, *Circulation* **107**, 1092 (2003).
- ⁷See (<http://mae.uta.edu/~bhan/research.html>).
- ⁸O. Amy, T. Farah, S. Kenneth, W. Alexander, and B. Stephen, *Opt. Express* **13**, 6597 (2005).
- ⁹P. L. Brannon and O. J. Blanchette, *Adv. Drug Delivery Rev.* **56**, 1649 (2004).
- ¹⁰R. K. Visaria, R. J. Griffin, B. W. Williams, E. S. Ebbini, G. F. Paciotti, C. W. Song, and J. C. Bischof, *Mol. Cancer Ther.* **5**, 1014 (2006).
- ¹¹P. Mazur, *Am. J. Physiol.* **143**, C125 (1984).
- ¹²R. V. Devireddy, D. J. Smith, and J. C. Bischof, *ASME J. Heat Transfer* **124**, 365 (2002).
- ¹³B. Rubinsky and D. E. Pegg, *Proc. R. Soc. London, Ser. B* **234**, 343 (1988).
- ¹⁴J. O. M. Karlsson, E. G. Cravalho, B. Rinkes, R. G. Tompkins, M. L. Yarmush, and M. Toner, *Biophys. J.* **65**, 2524 (1993).
- ¹⁵M. Toner, R. G. Tompkins, E. G. Cravalho, and M. L. Yarmush, *AIChE J.* **38**, 1512 (2004).
- ¹⁶D. Irimia and J. O. M. Karlsson, *Biophys. J.* **82**, 1858 (2002).
- ¹⁷G. Zhao, D. W. Luo, and D. Y. Gao, *AIChE J.* **52**, 2596 (2006).
- ¹⁸Z. S. Deng and J. Liu, *Numer. Heat Transfer, Part A* **46**, 587 (2004).
- ¹⁹H. Q. Xie, M. Fujii, and X. Zhang, *Int. J. Heat Mass Transfer* **48**, 2926 (2005).
- ²⁰X. Zhang, H. Gu, and M. Fujii, *J. Appl. Phys.* **100**, 044325 (2006).

- ²¹J. O. M. Karlsson, E. G. Cravalho, and M. Toner, *J. Appl. Phys.* **75**, 4442 (1994).
- ²²V. Vand, *J. Phys. Chem.* **52**, 277 (1948).
- ²³M. Toner, in *Advances in Low-Temperature Biology*, edited by P. L. Steponkus (JAI, London, 1993).
- ²⁴J. Liu, E. J. Woods, Y. Agca, E. S. Critser, and J. K. Critser, *Biol. Reprod.* **63**, 1303 (2000).
- ²⁵R. McCuen, *J. Hydrol.* **18**, 37 (1973).